

LARGE LANGUAGE MODELS TO ENHANCE BAYESIAN OPTIMIZATION

Tennison Liu*, Nicolás Astorga*, Nabeel Seedat & Mihaela van der Schaar

DAMTP, University of Cambridge

Cambridge, UK

{t1522,nja46,ns741,mv472}@cam.ac.uk

ABSTRACT

Bayesian optimization (BO) is a powerful approach for optimizing complex and expensive-to-evaluate black-box functions. Its importance is underscored in many applications, notably including hyperparameter tuning, but its efficacy depends on efficiently balancing exploration and exploitation. While there has been substantial progress in BO methods, striking this balance still remains a delicate process. In this light, we present **LLAMBO**, a novel approach that integrates the capabilities of large language models (LLM) within BO. At a high level, we frame the BO problem in natural language terms, enabling LLMs to iteratively propose promising solutions conditioned on historical evaluations. More specifically, we explore how combining contextual understanding, few-shot learning proficiency, and domain knowledge of LLMs can enhance various components of model-based BO. Our findings illustrate that **LLAMBO** is effective at zero-shot warmstarting, and improves surrogate modeling and candidate sampling, especially in the early stages of search when observations are sparse. Our approach is performed in context and does not require LLM finetuning. Additionally, it is modular by design, allowing individual components to be integrated into existing BO frameworks, or function cohesively as an end-to-end method. We empirically validate **LLAMBO**'s efficacy on the problem of hyperparameter tuning, highlighting strong empirical performance across a range of diverse benchmarks, proprietary, and synthetic tasks.

1 INTRODUCTION

Model-based optimization. Expensive black-box functions are common in many disciplines and applications including robotics (11, 35), experimental design (25), drug discovery (32), interface design (8) and, in machine learning for hyperparameter tuning (6, 34, 49). *Bayesian optimization* (BO) is a widely adopted and efficient model-based approach for globally optimizing these functions (31, 33). BO's effectiveness lies in its ability to operate based on a limited set of observations without the need for direct access to the objective function or its gradients. Broadly, BO uses observed data to construct a surrogate model as an approximation to the objective function, and then iteratively generates potentially good points, from which the acquisition function selects the one with the highest utility. This chosen point undergoes evaluation, and the cycle continues.

Challenges of search efficiency. For BO, the name of the game is efficient search, but the efficiency of this search largely depends on the quality of the surrogate model and its capacity to quickly identify high-potential regions (16). Given that BO is designated for scenarios with limited observations, constructing an accurate **surrogate model** with sparse observations is inherently challenging. Additionally, the model can be sensitive to misspecification, and even slight misrepresentations of the model can introduce undesired bias, skewing the **sampling of potential solutions** (24). A further challenge arises when considering the integration of **prior knowledge**, especially in effectively transferring knowledge about correlations in the optimization space to new tasks.

Dealing with limited data. At the core, these challenges pertain to the task of accurately *learning* the objective function and effectively *generating* candidate solutions with limited data. This scenario is typically framed as the *few-shot setting*, a context that demands swift learning and generalization

*Equal contribution

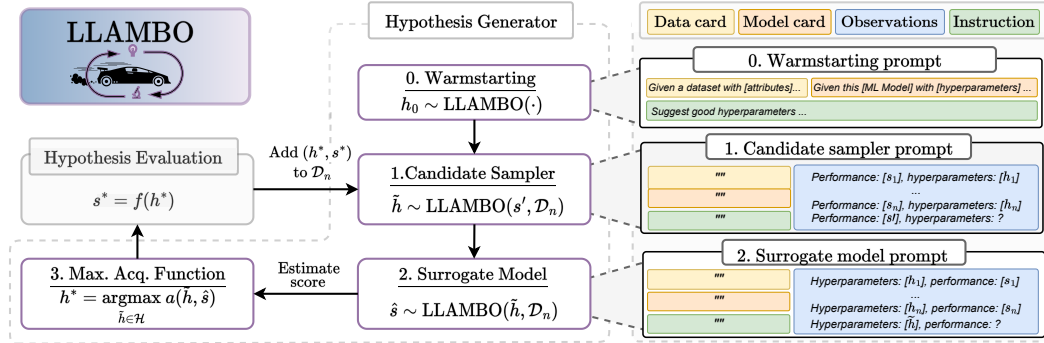


Figure 1: **Overview of LLAMBO.** In order: LLAMBO can initialize BO through ► **zero-shot warmstarting**, ► **efficiently sample candidate points** from high-potential regions given past observations and problem description, and ► **evaluate these candidate points via a surrogate model**.

from very few examples (57). Interestingly, such challenges of the few-shot paradigm align with the proficiencies of large language models (LLM). Specifically, contemporary LLMs such as GPT-3 and PaLM2, which have been pretrained on vast Internet-scale data, showcase an exceptional capacity to generalize from sparse data. This enables them to excel in few-shot prediction, generation (9, 13, 42), and contextual reasoning (59, 60). They achieve this remarkable sample-efficient performance, in part, by exploiting encoded prior knowledge (39, 47). Although the majority of these demonstrations were limited to the domain of natural language processing.

Key considerations. This study examines the potential of extending the capabilities of LLMs beyond standard natural language tasks to enhance model-based BO. Our approach is grounded in representing BO components using natural language, introducing novel methods to effectively capture LLM’s distinct strengths. This exploration gives rise to two key questions: **[Q1]** *Can LLMs, with their encoded knowledge and few-shot learning abilities, enhance key elements of BO, including the surrogate model and candidate point sampler?* **[Q2]** *How effectively can LLM-augmented BO components operate as a cohesive, end-to-end pipeline?* In answering these questions, we chose *hyperparameter tuning* (HPT) as our initial area of investigation. This is for two main reasons: firstly, the extensive knowledge potentially acquired by LLMs about HPT during pretraining makes it an ideal testbed to probe the applications of LLMs within BO. Secondly, HPT’s practical importance presents an avenue to translate the benefits of our approach into tangible outcomes.

Contributions. We present LLAMBO, a novel approach for integrating the capabilities of LLMs into BO. To understand the performance gains from this integration, we execute our study as an *investigation*, exploring the aforementioned questions. Our primary contributions are:

- We propose LLAMBO, a novel approach to enhance components of model-based BO with LLMs,
- We systematically investigate the enhancements of LLAMBO throughout the BO pipeline, showcasing significant improvements to ► **zero-shot warmstarting**, the ► **efficacy of the surrogate model**, and the ► **efficiency of candidate sampling**,
- We empirically investigated the end-to-end performance of LLAMBO for hyperparameter tuning, demonstrating strong performance on diverse benchmarks.

2 LLAMBO: LLMs TO ENHANCE BO

Figure 1 illustrates the architecture of the LLAMBO framework. Fundamentally, our methodology translates different processes in the BO pipeline into natural language. This allows the LLM to iteratively suggest solutions, informed both by the BO problem description and search history.

2.1 THE INTEGRATION OF LLMs INTO BO

Preliminaries. To aid with exposition, we introduce the following notation. Let us consider an objective function, $f : \mathcal{H} \rightarrow \mathcal{S}$, where $h \in \mathcal{H} \subseteq \mathbb{R}^d$ is the d -dimensional input, and $\mathcal{S} \in \mathbb{R}$ is the output space. We aim to find $h^* \in \mathcal{H}$ that minimizes this objective function:

$$h^* = \arg \min_{h \in \mathcal{H}} f(h)$$

where f is a costly black-box function without accessible gradient information. To overcome these limitations, BO employs a surrogate model to approximate f . We provide a comprehensive overview

of BO and related works in Appendix A. In general terms, a surrogate model can be viewed as a machine learning (ML) method producing the *predictive distribution* of s given h and some observed data $\mathcal{D}_n = \{(h_i, s_i)\}_{i=1}^n$:

$$p(s|h; \mathcal{D}_n) = \int_{\theta} p(s|h, \theta; \mathcal{D}_n) p(\theta|h; \mathcal{D}_n) d\theta$$

Here, the marginalization is over θ , a latent variable that captures the underlying structure between s and h . Specifically, $p(\theta|\mathcal{D}_n, h) \propto p(\mathcal{D}_n|\theta, h)p(\theta)$ describes the posterior distribution after observing some data, with $p(\theta)$ being the prior knowledge of this underlying structure. It is noteworthy to mention that different surrogate modeling approaches encode this prior differently: Gaussian Processes (GP) (49) embed priors through a distribution over functions, $p(f)$ while Bayesian neural networks incorporate it via priors within the weight space $p(w)$ (50). These priors can play a significant role, especially given the typically sparse observations in BO, and can fundamentally influence the model’s inference capabilities (5). However, in practice, many BO applications adopt non-informative priors, potentially missing out on incorporating valuable domain-specific knowledge. The challenge lies not just in the inclusion of prior knowledge, but also in accurately learning the associated predictive distribution with ML methods, especially in settings with limited observations.

Synergy of LLMs and BO. In this light, LLMs can offer significant enhancements due to the following capabilities: **(1) Prior knowledge:** Recently, (64) provided an explanation for LLM in-context learning (ICL) as performing implicit Bayesian inference (9). This raises the interesting prospect of using ICL to tap into an LLM’s encoded knowledge. In this framework, $p(\theta)$ represents the concepts related to the optimization problem and domain-specific correlations absorbed through pretraining (13, 48). **(2) In-context learning:** Learning robust, generalizable models given only limited observations is highly challenging. LLMs have demonstrated the capacity to generalize effectively from few-shot examples provided in context (9, 37, 61), an ability that can directly complement BO’s needs for sample-efficient exploration. **(3) Contextual understanding:** LLMs are adept at processing contextual information, especially via natural language (65). This offers a versatile interface to incorporate nuanced information about optimization tasks, search spaces, and other auxiliary details that can improve search performance.

Operationalizing this synergy. Despite the hypothesized advantages that LLMs can offer, effectively capitalizing on them in an *iterative optimization* framework like BO is challenging. Recently, (45) explored the use of LLM ICL for molecular optimization. While this work primarily focused on the surrogate model, we introduce novel methods for LLM enhancement of multiple components of BO and conduct a systematic investigation to understand the performance gains offered by this integration. Specifically, we employ ICL to enhance three key components of BO (Figure 1):

- **Warmstarting:** Warmstarting in BO is designed to initialize the optimization process with a pre-defined set of points, denoted as $\{h_i\}_{i=1}^n$ for n initial points. These points are evaluated first to build up a meaningful representation of the underlying function. In this context, we propose a strategy to identify promising initialization through *zero-shot* prompting.
- **Surrogate modeling:** The surrogate model, denoted as $p(s|h; \mathcal{D}_n)$, is an approximation of f and is trained using \mathcal{D}_n . We employ ICL by providing the optimization trajectories as few-shot examples. Specifically, we introduce two methods: a *discriminative* approach that produces regression estimates with uncertainty, and a *generative* approach that scores via binary classification.
- **Sampling candidates:** The sampling process proposes points $\{\tilde{h}_k\}_{k=1}^K$ that are considered for future evaluations. Drawing inspiration from TPE (6), we propose a mechanism to conditionally sample candidates based on a target objective value s' : $\tilde{h}_k \sim p(h|s'; \mathcal{D}_n)$. Here, we once again use ICL by providing the optimization history as few-shot examples.

Overview of investigation. Having outlined our approach for leveraging LLMs in BO, we now describe the structure of our investigative study. The framework is presented below, and centers around the two aforementioned questions [Q1-2]. We begin by analyzing each component in isolation, maintaining consistency in other factors, to distinctly evaluate its specific enhancements. We conclude our study with an assessment of LLAMBO’s performance as a fully integrated BO method.

Experimental setup. We conduct our investigations using Bayesmark, a continuous HPT benchmark (55). We use 25 *tasks* (encompassing 5 datasets and 5 ML models) where each task is evaluated over 10 seeds (see Section 6 for detailed experimental procedures). Additionally, we use OpenAI’s GPT-3.5 LLM in all our experiments (9).

| Section | Method | Goal and Method | Q's |
|-----------|--------------------|---|----------|
| Section 3 | Warmstarting | Enhancing optimization with warmstarting from LLM prior | [Q1] |
| Section 4 | Surrogate model | Improving quality of surrogate model in few-shot settings through ICL | [Q1] |
| Section 5 | Candidate sampling | Conditional sampling of high-potential points for desired s^* via ICL | [Q1] |
| Section 6 | End-to-end BO | Augmenting end-to-end BO performance | [Q1][Q2] |

2.2 BO PROMPT DESIGN

The proposed integrations are realized through structured natural language queries to the LLM. While the specifics of each query differ (e.g. for surrogate modeling and sampling), they are constructed from three essential elements.¹

- **Optimization problem description.** This includes information of the input space \mathcal{H} , the output space \mathcal{S} , and the objective function f . Specifically for HPT, this entails a `<MODEL CARD>`, describing the ML model being optimized (f), the hyperparameters (\mathcal{H}), and the scoring metric (\mathcal{S}). We also include a `<DATA CARD>` containing dataset attributes.
- **Optimization history.** The trajectory contains the sequence of points and scores observed during the optimization process, captured in \mathcal{D}_n . The observed points are provided as few-shot examples for ICL of the surrogate model and candidate point sampler.
- **Task instructions.** For each component under consideration (e.g. surrogate model), we include task-specific instructions on desired inference and guidelines on the format of the response.

3 WARMSTARTING THE BO PROCESS

Motivation. We start by analyzing whether LLMs can transfer prior knowledge about an optimization problem through warmstarting. While warmstarting can accelerate convergence by supplying more insightful initial points, conventional approaches require prior results collected from similar optimization problems (23, 30). This data collection can be resource-intensive and might not be feasible for certain applications. In contrast, we explore the use of LLMs for warmstarting as a more efficient and lightweight alternative, allowing the acquisition of warmstarting points without requiring data from related problems.

Method. LLAMBO employs *zero-shot prompting* to sample points for warmstarting. We explore three distinct settings, each providing different levels of information about the optimization problem. ► **No context:** the LLM is prompted to recommend good initial hyperparameters for a given ML model (through the `<MODEL CARD>`), but no dataset details are provided; ► **Partial context:** provides additional information about the dataset through the `<DATA CARD>`, including count of samples, features, the type of features (categorical *vs* continuous), and the learning task (e.g. classification); ► **Full context:** further augments the `<DATA CARD>` with information on marginal distributions, inter-feature correlations, and feature-label correlations.

Experimental setup. To evaluate the impact of warmstarting, we employ two widely adopted BO methods: Gaussian Processes (GP) (49) and Tree Parzen Estimator (TPE) (6). We compare these against random initialization techniques, namely Random, Sobol, and Latin Hypercube (HCube) sampling. Each search begins with 5 initialization points and proceeds for 25 trials, and we report average results over ten seeded searches. Our evaluation metrics focus on two aspects: *search performance* and the *diversity* of the initialization points. To assess search performance, we adopt the normalized regret metric, defined as $\min_{h \in \mathcal{H}_t} (f(h) - s_{min}^*) / (s_{max}^* - s_{min}^*)$, where \mathcal{H}_t denotes the points chosen up to trial t , and s_{min}^* and s_{max}^* represent the best and worse scores, respectively (2). To assess diversity, we use the generalized variance: $\det(\Sigma)$, with Σ being the covariance matrix of the hyperparameters.

¹For the complete prompts, please refer to Appendix B.

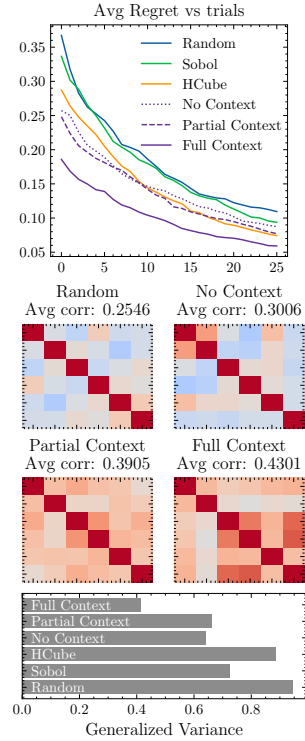


Figure 2: **Warmstarting.** (Top) average regret, (Middle) correlation of sampled initialization, (Bottom) diversity of different initialization methods.

Empirical insights. (1) Performance: Figure 2 (Top) visualizes the average regret across all tasks. We begin our analysis with a *sanity check*—namely, warmstarting using **no context** surpasses the performance of random initialization techniques. This verifies that our LLM possesses a basic understanding of good hyperparameter suggestions. Interestingly, we observe that providing additional information about the dataset improves the search performance when warmstarting for both **partial context** and **full context**. This is particularly prominent in the early stages of the search (i.e. trials < 5). However, these initial gains are maintained as the search progresses. **(1a) Correlations:** To explore deeper, we compute the correlation matrix of sampled warmstarting points depicted in (Middle) (with further analysis in Appendix E). Our findings reveal that the points recommended by the LLM exhibit considerably greater correlations between hyperparameters compared to those from random initialization. This indicates that such prompts are effectively *eliciting* the LLM’s prior knowledge about correlations within the problem space. More strikingly, the correlation matrices computed for different tasks reveal different correlation structures, suggesting that the LLM is dynamically adjusting its suggestions to different optimization problems. **(2) Diversity:** A closer look at the diversity of warmstarting points in (Bottom) reveals that their generalized variance is typically lower than that of randomly initialized points. This trend aligns with our expectations: higher correlations often lead to a decreased determinant of the covariance matrix due to the presence of ‘redundant’ information. Since random initialization methods sample each hyperparameter independently, they exhibit lower correlation levels, resulting in higher diversity.

💡 Warmstart initialization via zero-shot prompting is an efficient strategy to transfer knowledge about correlations in the optimization landscape, enhancing search performance.

4 SURROGATE MODELING

Motivation. Surrogate modeling, a core component of BO, aims to learn accurate representations of complex functions using only a limited set of evaluations. The efficacy of these models depends on their capacity to generalize and make accurate predictions from sparse observations, echoing the key tenets of few-shot learning. Recent studies have underscored LLM’s remarkable ability to perform few-shot learning in context (26, 64). Building on this, we propose two tailored approaches to surrogate modeling via ICL, aligning with BO’s primary modeling paradigms: a *discriminative* approach in Section 4.1 and a *generative* approach in Section 4.2.

4.1 DISCRIMINATIVE SURROGATE MODEL

One of the main approaches to surrogate modeling involves learning the conditional probability of the output s given the input h using data \mathcal{D}_n , expressed as $p(s|h; \mathcal{D}_n)$ —a *discriminative* approach. An effective surrogate model should produce an accurate mean prediction of the objective function’s central tendencies, and well-calibrated uncertainty estimates to balance exploration and exploitation.

Method. We serialize the observed *optimization trajectory* into natural text. For example, with h_i as an RF’s hyperparameters and s_i the accuracy, the serialization would read: “*max_depth is 15, min_samples_split is 0.5, ..., accuracy is 0.9*” (17, 28). These text representations, for all n observed samples, are concatenated into few-shot examples, symbolized as \mathcal{D}_n^{n1} . Here, we use the superscript $n1$ to mean representations of observations in natural text. Together with the problem description and query example h_k^{n1} , they form the input to the LLM. For each query, the LLM outputs a response: $(\hat{s}_k, p(\hat{s}_k))$, denoting the predicted score and associated probability, respectively: $(\hat{s}_k, p(\hat{s}_k)) = \text{LLAMBO}(h_k^{n1}, \mathcal{D}_n^{n1})$. To obtain probabilistic estimates, this prediction step is repeated K times, from which we compute the empirical mean and standard deviation. This Monte Carlo-based approach is termed LLAMBO (MC), and mirrors the method proposed in (45).

Our empirical observations revealed that the MC implementation often achieved suboptimal calibration of uncertainty estimates. After further explorations, we found the sensitivity to the ordering of in-context examples as a likely cause. As LLMs process inputs in a left-to-right manner, the predictions are sensitive to permutations within the prompt. This observation is consistent with findings around ordering sensitivity and biases of ICL in (36, 66). To enhance robustness, we introduce a shuffling mechanism that randomly permutes the few-shot examples within \mathcal{D}_n^{n1} . We acknowledge that while this approach is not grounded in principled probabilistic reasoning—similar to the popular SMAC method (34)—it can be an effective technique to obtain probabilistic estimates. This improved method is hereby referred to as LLAMBO.

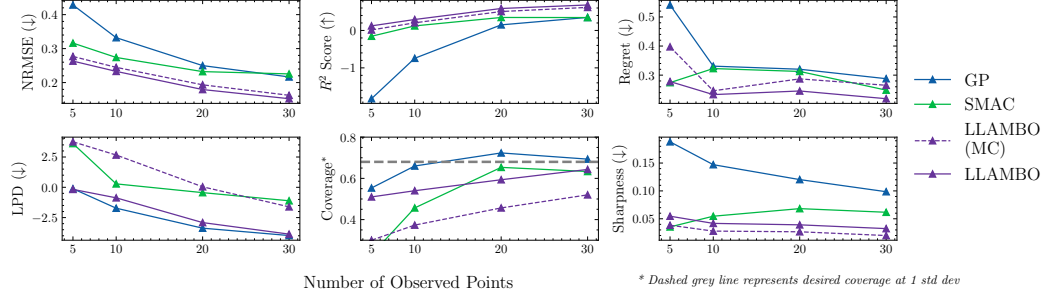


Figure 3: **Discriminative surrogate models.** (Top) prediction performance measured in NRMSE and R^2 , and regret; (Bottom) uncertainty calibration evaluated using LPD, coverage, and sharpness.

Experimental setup. We compare LLAMBO against GP and SMAC, two established surrogate models. We evaluate these probabilistic discriminative models via *prediction performance* and *uncertainty calibration*. For performance metrics, we use NRMSE (\downarrow) and R^2 (\uparrow). Calibration is assessed using the scoring rule, log predictive density (LPD) (\downarrow), empirical coverage (where the desired coverage for 1 standard deviation, assuming Gaussianity, is ≈ 0.68), and sharpness (\downarrow) (3). Our goal is to discern how the surrogate model’s efficacy evolves as the number of observed samples (n) varies. We evaluate each task when $n \in [5, 10, 20, 30]$, and we test predictions against 20 unseen points. We also include normalized regret, which is calculated with respect to the point selected from the unseen points using expected improvement (EI) (31).

Empirical insights. (1) **Prediction performance:** Figure 3 (Top) plots the NRMSE and R^2 against the number of observed samples. LLAMBO consistently outperforms in prediction across all sample counts, particularly with fewer observed samples. Moving on, we examine normalized regret: notably, all methods show increased regret at $n = 5$, this reflects greater uncertainty across unexplored regions, leading to heightened levels of exploration (and higher regret). For $n > 5$, LLAMBO attains lower regret, demonstrating better exploitation than other methods. (2) **Uncertainty quantification:** (Bottom) assesses uncertainty quantification. We find that, in this aspect, GPs, with their probabilistic grounding, produce the best uncertainty estimates, particularly in LPD and empirical coverage. GPs maintain good coverage even with a low number of samples, while LLAMBO only approaches similar performances as n increases. In this regard, our approach exhibits performance more similar to SMAC, a frequentist method that also makes use of empirical variance. Interestingly, we note that the sharpness of uncertainty intervals for GPs remains consistently higher, while in LLAMBO, the sharpness decreases as the coverage improves. This is likely due to the better prediction performance, enabling the predictions to be more confident (lower sharpness) while achieving improved empirical coverage. (3) **LLAMBO vs LLAMBO (MC)** The purely MC-driven approach exhibits subpar uncertainty calibration, evident through worse LPD and coverage metrics. Coupled with low sharpness values, this suggests the predictions are overly confident, tending to underestimate uncertainty. We also observe that LLAMBO consistently achieves better prediction performance. As such, empirical evidence supports that permuting few-shot examples, while straightforward in implementation, improves both uncertainty quantification and prediction performance, both critical aspects of balancing exploration and exploitation. (4) **Role of prior knowledge** Lastly, we investigate the importance of prior knowledge to LLAMBO’s few-shot performances. To this end, we introduce an ablation setting LLAMBO (UnInf) where the problem description (containing the <DATA CARD> and <MODEL CARD>) are omitted, and the hyperparameter names are substituted with “ X_i ”. Figure 4 reveals better prediction performance and calibration when compared to the uninformative ablation. This reveals the crucial role of prior knowledge in enhancing surrogate modeling, especially in few-shot settings (28, 64).

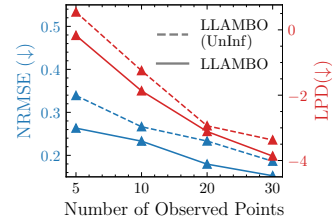


Figure 4: **Ablation.** LLAMBO (UnInf) omits problem description and hyperparameter names.

💡 Discriminative surrogate models implemented through ICL can produce effective regression estimates with uncertainty, although there is a tradeoff of stronger prediction performance with worse calibration than probabilistic methods. The LLM’s encoded prior is crucial to improving the efficacy of such surrogate models.

4.2 GENERATIVE SURROGATE MODEL

Method. An alternative approach to surrogate modelling is to learn the *generative process* of inputs given the output, represented as $p(h|s; \mathcal{D}_n)$. This approach is exemplified in TPE-based methods (6), which constructs two hierarchical processes formulated as $p(h|s; \mathcal{D}_n) = l(h)$ if $s < \tau$ else $g(h)$. Here $l(h)$ is the generative model of *good* points, and $g(h)$ is the model for *bad* points. In this context, good points refer to those with score $s < \tau$, where τ defines the threshold of the top γ quantile of observed s . Conversely, bad points correspond to scores $s \geq \tau$, or the bottom $1 - \gamma$ quantile of results. TPE evaluates each point using the acquisition function $a(h) \propto l(h)/g(h)$, which intuitively scores each point based on their likelihood of being good over bad. At first glance, it appears challenging to learn the two densities $l(h)$ and $g(h)$ directly with an LLM.

To address this, we employ Bayes’ rule, transforming the density ratio estimation into probabilistic *binary classification* (53). Complete exposition can be found in Appendix D. In essence, the scoring function can be equivalently written as $a(h) = \gamma^{-1}p(s < \tau|h)$, which is proportional to $p(s < \tau|h)$, the probability of an input producing good scores. Using this reformulation, we can now estimate the score $a(h)$ through ICL, by obtaining the probabilistic classification $p(s < \tau|h)$. We recategorize the observed samples, such that $z_i = \mathbb{1}(s_i < \tau)$, meaning the label is 1 if the performance exceeds the desired threshold. As before, we transform the observed samples to text $\mathcal{D}_n^{n1} := \{(h_i^{n1}, z_i^{n1})\}^n$, obtaining K predictions from the LLM, $(\hat{z}_k, p(\hat{z}_k)) = \text{LLAMBO}(h_k^{n1}, \mathcal{D}_n^{n1})$, and computing empirical average to estimate $a(h)$.

Experimental setup. We compare the performance of the proposed generative surrogate model vs two variants of TPE: TPE (Ind) which models each dimension independently, and TPE (Multi) which models joint multivariate densities (21). We evaluate the *scoring performance* and *regret* attained by these surrogate models. To assess scoring performance, we report the correlation between estimated scores $a(h)$ with ground-truth scores. Additionally, we calculate regret with respect to the point that was assigned the highest score. As before, we evaluate each task when $n \in [5, 10, 20, 30]$, and we test predictions against 20 unseen samples.

Empirical insights. (1) Scoring performance. Figure 5 (Top) visualizes the correlation between surrogate model predicted scores and ground truth objective values. We observe that LLAMBO achieves notably higher correlations, especially at $n=5$, where the TPE variants generated scores that are only weakly correlated with the ground truth performance. We note that as n increases, the correlation of baseline scores improves, but LLAMBO is still superior.

(2) Regret (Bottom) examines the regret of the point picked from the 20 available points. We find that while all methods show higher regret at low sample sizes when levels of exploration are higher, LLAMBO quickly identifies good regions in the search space, leading to lower regret as n increases.

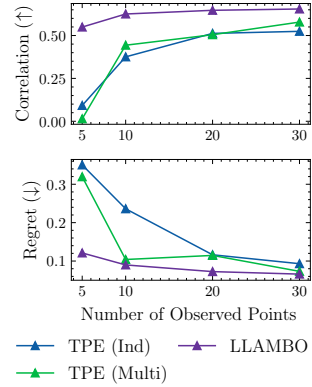


Figure 5: **Generative surrogate model. (Top)** score correlation and **(Bottom)** regret.

💡 *Generative surrogate modeling via ICL predicts scores that are more highly correlated with ground-truth scores, leading to better identification of high-potential points.*

5 SAMPLING OF CANDIDATE POINTS

Motivation. The sampling of candidate points is another crucial component of BO, as high-potential points can speed up convergence to the optimal solution. In this context, we present a novel mechanism to conditionally generate candidate points based on desired objective values through ICL.

Method. Our proposed sampling mechanism draws inspiration from TPE. While TPE focuses on sampling candidate points, denoted as \tilde{h}_m , from ‘good’ regions in the search space (i.e. $\tilde{h}_m \sim l(h) = p(h|s < \tau; \mathcal{D}_n)$), we sample from regions of high potential by directly conditioning on a desired objective value s' : $\tilde{h}_m \sim p(h|s'; \mathcal{D}_n)$. This distinction is fundamental as it allows us to target specific objective values, something TPE’s binary categorization cannot achieve. The few-shot generation capabilities of LLMs are crucial here, as learning such a conditional generator through conventional means poses significant challenges due to the limited number of observations.

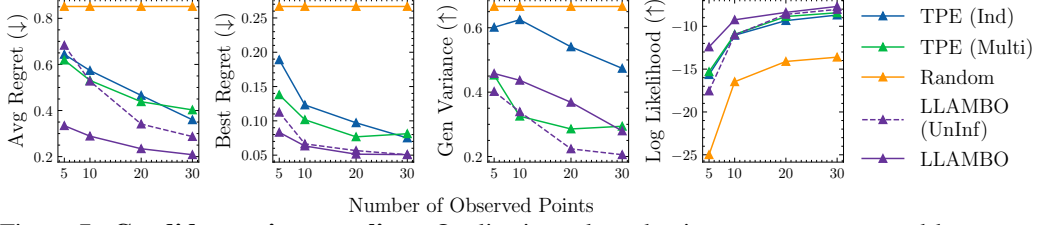


Figure 7: **Candidate point sampling.** Quality is evaluated using average regret and best regret. Diversity is assessed using generalized and log-likelihood.

We define the desired objective value using the equation: $s' = s_{min} - \alpha \times (s_{max} - s_{min})$, where s_{max} and s_{min} are the worst and best objective values observed up until that point. Intuitively, s' is defined relative to the best objective value, with the difference proportional to the observed variability in s . The exact value is controlled by α , the *exploration* hyperparameter. A positive α sets s' to improve over s_{min} . Here, we are essentially extrapolating, which cannot be achieved through conventional TPE. Conversely, a negative α (i.e. $-1 \leq \alpha < 0$) results in a more conservative target value that is within the observed objective value range. To operationalize this, we implement $p(h|s'; \mathcal{D}_n)$ through ICL. We generate M candidate points independently, i.e. $\tilde{h}_k \sim \text{LLAMBO}(s', \mathcal{D}_n^{\perp})$, after which, we select the point that maximizes the acquisition function as the point to evaluate next. Thus, we adopt a sampling-based approach to optimize the acquisition function.

Experimental setup. We compare our proposed sampler against TPE (Ind), TPE (Multi), and random sampling (Random). As before, we also include ablation of our method `LLAMBO (UnInf)`, which omits problem description and hyperparameter names. Our analysis examines two aspects: *candidate point quality* and *diversity*. To evaluate quality, we compute the average regret (\downarrow) and best regret (\downarrow) among the M sampled points (2). For assessing diversity, we use generalized variance (\uparrow) to evaluate the spread of candidate points and log-likelihood (\uparrow) to assess the probability of candidate points being sampled from observed points. We start by investigating the effect of α on sampling performance. Then, following the experimental procedure outlined previously, we evaluate sampling performance when a different number of observations are available.

Empirical insights. (1) Effect of α : In Figure 6, we observe that as α increases from -0.5 to 0 , both average regret and best regret improves. However, as α increases beyond 0 , the average regret increases as the candidate points are increasingly sampled from beyond the observed distribution, compromising the reliability of these points. Interestingly, the optimal best regret emerges at $\alpha=0.01$, hinting at our mechanism’s ability to extrapolate from observed distributions. The generalized variance decreases with increasing α , this is reasonable as the candidate points are sampled from smaller regions in the search space. Similarly, the log-likelihood decreases as α increases, as the points are increasingly sampled away from observed points. To confirm that this is indeed the case, we visually examine t-SNE projections of sampled points, localizing them with respect to good (top 20% of samples) and bad points (56). We note that when $\alpha=-0.2$, the candidate points cover a similar region as good points, but when $\alpha=0.01$, the sampled points are observed outside the regions of good points. **(2) Quality:** Figure 7 compares the quality of our sampled points against baselines, with our method set at $\alpha=-0.2$. We observe that `LLAMBO` consistently achieves the lowest average and best regret as n varies, but is especially notable at $n = 5$. This gain is also present when compared against the ablation, suggesting the crucial role of prior knowledge in proposing high-potential candidates. **(3) Diversity:** An examination of generalized variance reveals that TPE (Ind) proposes more diverse points. In contrast, the spread of `LLAMBO`-sampled points is similar to that achieved by TPE (Multi). This is reasonable, as both `LLAMBO` and TPE (Multi) consider correlations between hyperparameters, while TPE (Ind) models each dimension independently (and higher correlation decreases generalized variance). Furthermore, the log-likelihood of `LLAMBO` proposed points are the highest, indicating that they are more plausible given the observed points.

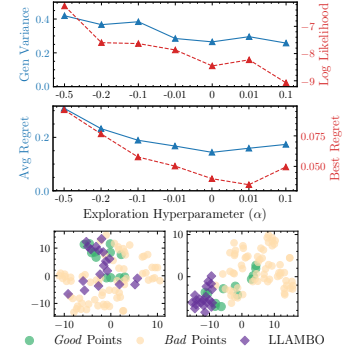


Figure 6: **(Top)** quality and diversity of points sampled with different α . **(Bottom)** projection of sampled points at $\alpha=-0.2$ and $\alpha=0.01$.

💡 *Sampling candidate points by direct conditioning on desired target value can generate high-quality points, although this can sacrifice diversity among sampled points. The α exploration hyperparameter allows balancing of this trade-off.*

6 END-TO-END DEMONSTRATION OF LLAMBO

Motivation. Having examined the integration of LLMs into key components of BO, we now holistically evaluate the performance of LLAMBO as a stand-alone model-based BO algorithm. Here, we instantiate LLAMBO with our discriminative surrogate model, as this is the most classic form of surrogate modeling.²

Experimental setup. HPT tasks. We evaluate end-to-end performance on Bayesmark (55), a continuous HPT benchmark. We utilize all 5 included datasets and 5 ML models, including RandomForest, SVM, DecisionTree, MLP, and AdaBoost. Additionally, we introduce 3 proprietary and 2 synthetic datasets into the benchmark—these are datasets for which the LLM would not have seen during pretraining, and thus serve to check for any memorization concerns. This results in a total of 50 HPT tasks (where a *task* is a dataset-model pair). For each task, we executed 5 seeded searches (resulting in a total of 250 HPT searches), where each search proceeded for 25 trials. **Baselines.** We compare LLAMBO against 4 established baselines commonly used in production, namely GP-DKL (62), SKOpt (GP) (41), Optuna (TPE) (1), and SMAC3 (RF) (34). We describe complete experimental details in Appendix C and include results on additional baselines in Appendix E. To ensure a fair comparison, we do not use warmstarting and initialize all methods with the same set of 5 randomly sampled points in each run.

Empirical insights. (1) Performance: Figure 8 shows the average regrets across all HPT tasks on both public Bayesmark datasets, and private and synthetic datasets. We note that in both settings, LLAMBO achieves the best tuning performance. Additionally, we observe that, consistent with prior findings, LLAMBO excels in earlier stages of the search, when fewer observations are available. **(2) Additional results:** In Appendix E, we show the individual task search results by task metric, average regret, and average rank in Figures 19 to 21 respectively. We also tabulate the average rank achieved for each ML method in Tables 1 and 2.

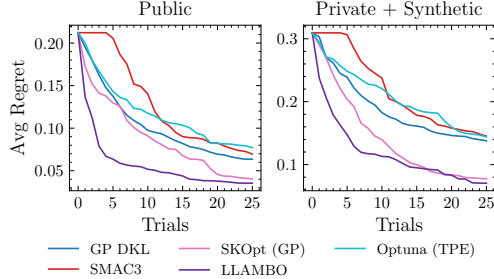


Figure 8: **End-to-end performance of LLAMBO.** (Left) average regret on public datasets and (Right) private and synthetic datasets evaluated on Bayesmark.

7 DISCUSSIONS

In summary, we introduced LLAMBO, a novel approach that integrated LLM capabilities to enhance the efficacy of model-based BO. Our approach introduced three specific enhancements: ► **zero-shot warmstarting** to initialize search, generative and discriminative ► **surrogate models** of the objective function via ICL, and a ► **candidate point sampler** that can conditionally generate for specific target values. Our investigative study on the problem of HPT uncovered performance improvements across all three integrations, which was especially notable when fewer samples were available. Additionally, we found that LLAMBO to be an effective stand-alone BO method, exemplified through superior performance on diverse benchmarks.

Limitations & future works. While LLAMBO does not perform any finetuning, performing inference through LLMs incurs a much larger computational footprint than traditional BO algorithms. Our findings indicated that LLAMBO trades off this computational complexity for improved sample efficiency, an especially desirable property in black-box optimization tasks. This suggests the potential fusion of LLAMBO with more computationally efficient methods. For instance, deploying LLAMBO in earlier stages of the search, or only leveraging an individual component to complement existing BO frameworks. Additionally, the performance of LLAMBO leans partly on domain expertise contained in LLMs, a potential constraint in domains where LLM expertise is sparse. In these instances, domain-specific finetuning could be the solution.

²Due to budget constraints, we evaluate the generative surrogate model for limited runs, see Appendix E

ETHICS AND REPRODUCIBILITY STATEMENTS

Ethics. In this work, we evaluate both public benchmarks and private datasets. The private datasets are *de-identified* and used in accordance with the guidance of the respective data providers. We follow recommendations to use the Azure OpenAI service when using GPT models, where via the agreement we ensure the medical data is not sent for human review or stored, hence respecting the guidelines given by the dataset providers.

Reproducibility. Experimental investigations are described in Sections 3-6 with further details of the method, experimental setup, and datasets included in Appendix C. Code will be released upon acceptance.

REFERENCES

- [1] Takuya Akiba, Shotaro Sano, Toshihiko Yanase, Takeru Ohta, and Masanori Koyama. Optuna: A next-generation hyperparameter optimization framework. In *Proceedings of the 25th ACM SIGKDD International Conference on Knowledge Discovery and Data Mining*, 2019.
- [2] Sebastian Pineda Arango, Hadi Samer Jomaa, Martin Wistuba, and Josif Grabocka. Hpo-b: A large-scale reproducible benchmark for black-box hpo based on openml. In *Thirty-fifth Conference on Neural Information Processing Systems Datasets and Benchmarks Track (Round 2)*, 2021.
- [3] Paul D Arendt, Daniel W Apley, and Wei Chen. Quantification of model uncertainty: Calibration, model discrepancy, and identifiability. *Journal of mechanical design*, 134(10), 2012.
- [4] Rémi Bardenet, Mátyás Brendel, Balázs Kégl, and Michele Sebag. Collaborative hyperparameter tuning. In *International conference on machine learning*, pages 199–207. PMLR, 2013.
- [5] James O Berger. *Statistical decision theory and Bayesian analysis*. Springer Science & Business Media, 2013.
- [6] James Bergstra, Rémi Bardenet, Yoshua Bengio, and Balázs Kégl. Algorithms for hyperparameter optimization. *Advances in neural information processing systems*, 24, 2011.
- [7] James Bergstra, Brent Komer, Chris Eliasmith, Dan Yamins, and David D. Cox. Hyperopt: A python library for model selection and hyperparameter optimization. *Computational Science & Discovery*, 8(1):014008, 2015.
- [8] Eric Brochu, Tyson Brochu, and Nando De Freitas. A bayesian interactive optimization approach to procedural animation design. In *Proceedings of the 2010 ACM SIGGRAPH/Eurographics Symposium on Computer Animation*, pages 103–112, 2010.
- [9] Tom Brown, Benjamin Mann, Nick Ryder, Melanie Subbiah, Jared D Kaplan, Prafulla Dhariwal, Arvind Neelakantan, Pranav Shyam, Girish Sastry, Amanda Askell, et al. Language models are few-shot learners. *Advances in neural information processing systems*, 33:1877–1901, 2020.
- [10] Roberto Calandra, Jan Peters, Carl Edward Rasmussen, and Marc Peter Deisenroth. Manifold gaussian processes for regression. In *2016 International joint conference on neural networks (IJCNN)*, pages 3338–3345. IEEE, 2016.
- [11] Roberto Calandra, André Seyfarth, Jan Peters, and Marc Peter Deisenroth. Bayesian optimization for learning gaits under uncertainty: An experimental comparison on a dynamic bipedal walker. *Annals of Mathematics and Artificial Intelligence*, 76:5–23, 2016.
- [12] Yutian Chen, Xingyou Song, Chansoo Lee, Zi Wang, Richard Zhang, David Dohan, Kazuya Kawakami, Greg Kochanski, Arnaud Doucet, Marc aurelio Ranzato, et al. Towards learning universal hyperparameter optimizers with transformers. *Advances in Neural Information Processing Systems*, 35:32053–32068, 2022.

- [13] Aakanksha Chowdhery, Sharan Narang, Jacob Devlin, Maarten Bosma, Gaurav Mishra, Adam Roberts, Paul Barham, Hyung Won Chung, Charles Sutton, Sebastian Gehrmann, et al. Palm: Scaling language modeling with pathways. *arXiv preprint arXiv:2204.02311*, 2022.
- [14] Alexander Cowen-Rivers, Wenlong Lyu, Rasul Tutunov, Zhi Wang, Antoine Grosnit, Ryan Rhys Griffiths, Alexandre Maravel, Jianye Hao, Jun Wang, Jan Peters, and Haitham Bou Ammar. Hebo: Pushing the limits of sample-efficient hyperparameter optimisation. *Journal of Artificial Intelligence Research*, 74, 07 2022.
- [15] Alexander I Cowen-Rivers, Wenlong Lyu, Rasul Tutunov, Zhi Wang, Antoine Grosnit, Ryan Rhys Griffiths, Alexandre Max Maraval, Hao Jianye, Jun Wang, Jan Peters, et al. Hebo: Pushing the limits of sample-efficient hyper-parameter optimisation. *Journal of Artificial Intelligence Research*, 74:1269–1349, 2022.
- [16] Thomas Desautels, Andreas Krause, and Joel W Burdick. Parallelizing exploration-exploitation tradeoffs in gaussian process bandit optimization. *Journal of Machine Learning Research*, 15:3873–3923, 2014.
- [17] T. Dinh, Y. Zeng, R. Zhang, Z. Lin, M. Gira, S. Rajput, J. Yong Sohn, D. Papailiopoulos, and K. Lee. Lift: Language-interfaced fine-tuning for non-language machine learning tasks. In A. H. Oh, A. Agarwal, D. Belgrave, and K. Cho, editors, *Advances in Neural Information Processing Systems*, 2022.
- [18] Máire A Duggan, William F Anderson, Sean Altekruze, Lynne Penberthy, and Mark E Sherman. The surveillance, epidemiology and end results (SEER) program and pathology: towards strengthening the critical relationship. *The American Journal of Surgical Pathology*, 40(12):e94, 2016.
- [19] David Duvenaud. *Automatic model construction with Gaussian processes*. PhD thesis, 2014.
- [20] David Eriksson, Michael Pearce, Jacob Gardner, Ryan D Turner, and Matthias Poloczek. Scalable global optimization via local Bayesian optimization. In *Advances in Neural Information Processing Systems*, pages 5496–5507, 2019.
- [21] Stefan Falkner, Aaron Klein, and Frank Hutter. Bohb: Robust and efficient hyperparameter optimization at scale. In *International conference on machine learning*, pages 1437–1446. PMLR, 2018.
- [22] Matthias Feurer, Benjamin Letham, and Eytan Bakshy. Scalable meta-learning for bayesian optimization. *arXiv preprint arXiv:1802.02219*, 2018.
- [23] Matthias Feurer, Jost Tobias Springenberg, and Frank Hutter. Initializing bayesian hyperparameter optimization via meta-learning. In *Twenty-Ninth AAAI Conference on Artificial Intelligence*, 2015.
- [24] Peter I Frazier. A tutorial on bayesian optimization. *arXiv preprint arXiv:1807.02811*, 2018.
- [25] Stewart Greenhill, Santu Rana, Sunil Gupta, Pratibha Vellanki, and Svetha Venkatesh. Bayesian optimization for adaptive experimental design: A review. *IEEE access*, 8:13937–13948, 2020.
- [26] Chi Han, Ziqi Wang, Han Zhao, and Heng Ji. In-context learning of large language models explained as kernel regression. *arXiv preprint arXiv:2305.12766*, 2023.
- [27] Ali Hebbal, Loïc Brevault, Mathieu Balesdent, Ei-Ghazali Taibi, and Nouredine Melab. Efficient global optimization using deep gaussian processes. In *2018 IEEE Congress on evolutionary computation (CEC)*, pages 1–8. IEEE, 2018.
- [28] Stefan Hagselmann, Alejandro Buendia, Hunter Lang, Monica Agrawal, Xiaoyi Jiang, and David Sontag. Tabllm: Few-shot classification of tabular data with large language models. In *International Conference on Artificial Intelligence and Statistics*, pages 5549–5581. PMLR, 2023.

- [29] Frank Hutter, Holger H Hoos, and Kevin Leyton-Brown. Sequential model-based optimization for general algorithm configuration. In *International Conference on Learning and Intelligent Optimization*, pages 507–523. Springer, 2011.
- [30] Hadi S Jomaa, Lars Schmidt-Thieme, and Josif Grabocka. Dataset2vec: Learning dataset meta-features. *Data Mining and Knowledge Discovery*, 35(3):964–985, 2021.
- [31] Donald R Jones, Matthias Schonlau, and William J Welch. Efficient global optimization of expensive black-box functions. *Journal of Global optimization*, 13:455–492, 1998.
- [32] Ksenia Korovina, Sailun Xu, Kirthevasan Kandasamy, Willie Neiswanger, Barnabas Poczos, Jeff Schneider, and Eric Xing. Chembo: Bayesian optimization of small organic molecules with synthesizable recommendations. In *International Conference on Artificial Intelligence and Statistics*, pages 3393–3403. PMLR, 2020.
- [33] HJ Kushner. A new method of locating the maximum point of an arbitrary multipeak curve in the presence of noise. *Journal of Basic Engineering*, 86(1):97–106, 1964.
- [34] Marius Lindauer, Katharina Eggensperger, Matthias Feurer, André Biedenkapp, Difan Deng, Carolin Benjamins, Tim Ruhkopf, René Sass, and Frank Hutter. Smac3: A versatile bayesian optimization package for hyperparameter optimization. *The Journal of Machine Learning Research*, 23(1):2475–2483, 2022.
- [35] Daniel J Lizotte, Tao Wang, Michael H Bowling, Dale Schuurmans, et al. Automatic gait optimization with gaussian process regression. In *IJCAI*, volume 7, pages 944–949, 2007.
- [36] Yao Lu, Max Bartolo, Alastair Moore, Sebastian Riedel, and Pontus Stenetorp. Fantastically ordered prompts and where to find them: Overcoming few-shot prompt order sensitivity. In *Proceedings of the 60th Annual Meeting of the Association for Computational Linguistics (Volume 1: Long Papers)*, pages 8086–8098, 2022.
- [37] Suvir Mirchandani, Fei Xia, Pete Florence, Brian Ichter, Danny Driess, Montserrat Gonzalez Arenas, Kanishka Rao, Dorsa Sadigh, and Andy Zeng. Large language models as general pattern machines. *arXiv preprint arXiv:2307.04721*, 2023.
- [38] Samuel Müller, Matthias Feurer, Noah Hollmann, and Frank Hutter. Pfns4bo: In-context learning for bayesian optimization. 2023.
- [39] Long Ouyang, Jeffrey Wu, Xu Jiang, Diogo Almeida, Carroll Wainwright, Pamela Mishkin, Chong Zhang, Sandhini Agarwal, Katarina Slama, Alex Ray, et al. Training language models to follow instructions with human feedback. *Advances in Neural Information Processing Systems*, 35:27730–27744, 2022.
- [40] Prostate Cancer UK PCUK. Cutract. <https://prostatecanceruk.org>, 2019.
- [41] F. Pedregosa, G. Varoquaux, A. Gramfort, V. Michel, B. Thirion, O. Grisel, M. Blondel, P. Prettenhofer, R. Weiss, V. Dubourg, J. Vanderplas, A. Passos, D. Cournapeau, M. Brucher, M. Perrot, and E. Duchesnay. Scikit-learn: Machine learning in Python. *Journal of Machine Learning Research*, 12:2825–2830, 2011.
- [42] Guilherme Penedo, Quentin Malartic, Daniel Hesslow, Ruxandra Cojocaru, Alessandro Capelli, Hamza Alobeidli, Baptiste Pannier, Ebtesam Almazrouei, and Julien Launay. The refinedweb dataset for falcon llm: outperforming curated corpora with web data, and web data only. *arXiv preprint arXiv:2306.01116*, 2023.
- [43] Stuart J Pocock, Cono A Ariti, John JV McMurray, Aldo Maggioni, Lars Køber, Iain B Squire, Karl Swedberg, Joanna Dobson, Katrina K Poppe, Gillian A Whalley, et al. Predicting survival in heart failure: a risk score based on 39 372 patients from 30 studies. *European Heart Journal*, 34(19):1404–1413, 2013.
- [44] Matthias Poloczek, Jialei Wang, and Peter I Frazier. Warm starting bayesian optimization. In *2016 Winter Simulation Conference (WSC)*, pages 770–781. IEEE, 2016.

- [45] Mayk Caldas Ramos, Shane S Michtavy, Marc D Porosoff, and Andrew D White. Bayesian optimization of catalysts with in-context learning. *arXiv preprint arXiv:2304.05341*, 2023.
- [46] Carl Edward Rasmussen, Christopher KI Williams, et al. *Gaussian processes for machine learning*, volume 1. Springer, 2006.
- [47] Victor Sanh, Albert Webson, Colin Raffel, Stephen Bach, Lintang Sutawika, Zaid Alyafeai, Antoine Chaffin, Arnaud Stiegler, Arun Raja, Manan Dey, M Saiful Bari, Canwen Xu, Urmish Thakker, Shanya Sharma Sharma, Eliza Szczechla, Taewoon Kim, Gunjan Chhablani, Nihal Nayak, Debajyoti Datta, Jonathan Chang, Mike Tian-Jian Jiang, Han Wang, Matteo Manica, Sheng Shen, Zheng Xin Yong, Harshit Pandey, Rachel Bawden, Thomas Wang, Trishala Neeraj, Jos Rozen, Abheesht Sharma, Andrea Santilli, Thibault Fevry, Jason Alan Fries, Ryan Teehan, Teven Le Scao, Stella Biderman, Leo Gao, Thomas Wolf, and Alexander M Rush. Multitask prompted training enables zero-shot task generalization. In *International Conference on Learning Representations*, 2022.
- [48] Karan Singhal, Shekoofeh Azizi, Tao Tu, S Sara Mahdavi, Jason Wei, Hyung Won Chung, Nathan Scales, Ajay Tanwani, Heather Cole-Lewis, Stephen Pfohl, et al. Large language models encode clinical knowledge. *Nature*, pages 1–9, 2023.
- [49] Jasper Snoek, Hugo Larochelle, and Ryan P Adams. Practical bayesian optimization of machine learning algorithms. *Advances in neural information processing systems*, 25, 2012.
- [50] Jasper Snoek, Oren Rippel, Kevin Swersky, Ryan Kiros, Nadathur Satish, Narayanan Sundaram, Mostofa Patwary, Prabhat, and Ryan P. Adams. Scalable bayesian optimization using deep neural networks. In *International Conference on Machine Learning*, pages 2171–2180, 2015.
- [51] Jost Tobias Springenberg, Aaron Klein, Stefan Falkner, and Frank Hutter. Bayesian optimization with robust bayesian neural networks. In D. Lee, M. Sugiyama, U. Luxburg, I. Guyon, and R. Garnett, editors, *Advances in Neural Information Processing Systems*, volume 29. Curran Associates, Inc., 2016.
- [52] Niranjan Srinivas, Andreas Krause, Sham Kakade, and Matthias Seeger. Gaussian process optimization in the bandit setting: no regret and experimental design. In *Proceedings of the 27th International Conference on Machine Learning*, pages 1015–1022, 2010.
- [53] Masashi Sugiyama, Taiji Suzuki, and Takafumi Kanamori. *Density ratio estimation in machine learning*. Cambridge University Press, 2012.
- [54] Kevin Swersky, Jasper Snoek, and Ryan P Adams. Multi-task bayesian optimization. *Advances in neural information processing systems*, 26, 2013.
- [55] Uber. Uber/bayesmark: Benchmark framework to easily compare bayesian optimization methods on real machine learning tasks, 2020.
- [56] Laurens Van der Maaten and Geoffrey Hinton. Visualizing data using t-sne. *Journal of machine learning research*, 9(11), 2008.
- [57] Yaqing Wang, Quanming Yao, James T Kwok, and Lionel M Ni. Generalizing from a few examples: A survey on few-shot learning. *ACM computing surveys (csur)*, 53(3):1–34, 2020.
- [58] S. Watanabe. Tree-structured Parzen estimator: Understanding its algorithm components and their roles for better empirical performance. *arXiv preprint arXiv:2304.11127*, 2023.
- [59] Jason Wei, Yi Tay, Rishi Bommasani, Colin Raffel, Barret Zoph, Sebastian Borgeaud, Dani Yogatama, Maarten Bosma, Denny Zhou, Donald Metzler, et al. Emergent abilities of large language models. *arXiv preprint arXiv:2206.07682*, 2022.
- [60] Jason Wei, Xuezhi Wang, Dale Schuurmans, Maarten Bosma, Fei Xia, Ed Chi, Quoc V Le, Denny Zhou, et al. Chain-of-thought prompting elicits reasoning in large language models. *Advances in Neural Information Processing Systems*, 35:24824–24837, 2022.

- [61] Jerry Wei, Jason Wei, Yi Tay, Dustin Tran, Albert Webson, Yifeng Lu, Xinyun Chen, Hanxiao Liu, Da Huang, Denny Zhou, et al. Larger language models do in-context learning differently. *arXiv preprint arXiv:2303.03846*, 2023.
- [62] Andrew Gordon Wilson, Zhiting Hu, Ruslan Salakhutdinov, and Eric P. Xing. Deep kernel learning. In Arthur Gretton and Christian C. Robert, editors, *Proceedings of the 19th International Conference on Artificial Intelligence and Statistics*, volume 51 of *Proceedings of Machine Learning Research*, pages 370–378, Cadiz, Spain, 09–11 May 2016. PMLR.
- [63] Martin Wistuba and Josif Grabocka. Few-shot bayesian optimization with deep kernel surrogates. In *International Conference on Learning Representations*, 2021.
- [64] Sang Michael Xie, Aditi Raghunathan, Percy Liang, and Tengyu Ma. An explanation of in-context learning as implicit bayesian inference. In *International Conference on Learning Representations*, 2022.
- [65] Chengrun Yang, Xuezhi Wang, Yifeng Lu, Hanxiao Liu, Quoc V Le, Denny Zhou, and Xinyun Chen. Large language models as optimizers. *arXiv preprint arXiv:2309.03409*, 2023.
- [66] Zihao Zhao, Eric Wallace, Shi Feng, Dan Klein, and Sameer Singh. Calibrate before use: Improving few-shot performance of language models. In *International Conference on Machine Learning*, pages 12697–12706. PMLR, 2021.

A BAYESIAN OPTIMIZATION BACKGROUND

A.1 PRELIMINARIES

Consider an objective function: $f : \mathcal{H} \rightarrow \mathcal{S}$, where $h \in \mathcal{H}$ is the input (which could be \mathbb{R}^d for d -dimensional input) and $\mathcal{S} \in \mathbb{R}$ is the output space. We aim to find $h^* \in \mathcal{H}$ that minimizes the objective function:

$$h^* = \arg \min_{h \in \mathcal{H}} f(h)$$

However, f is assumed to be a black-box function and evaluations of f might be expensive. To address these limitations, BO is a promising method that constructs a surrogate model to approximate f and iteratively proposes potential points. In more detail, the core components are:

1. **Surrogate model:** BO methods typically construct a surrogate approximation of f using available samples. We denote the surrogate model $p(s|h; \mathcal{D}_n)$, where $\mathcal{D}_n := \{(h_i, s_i)\}_{i=1}^n$ are the n observed input-output pairs. Some commonly used models include the Gaussian Process (GP) (49), and random forests (SMAC) (34). An alternative approach is the Tree Parzen Estimator (TPE) (6) which uses two hierarchical processes $l(x)$ and $g(x)$ to model input distributions when the objective function is above or below a specified quantile τ : $p(h|s; \mathcal{D}_n) = l(h)$ if $h < \tau$, else $g(h)$.
2. **Candidate point sampler:** The sampler proposes a set of candidate points $\tilde{\mathcal{H}} := \{\tilde{h}_i\}_{i=1}^K$ to query next. We denote the sampler $p(h|\mathcal{D}_n)$, where each candidate point is sampled independently $\tilde{h}_i \sim p(h|\mathcal{D}_n)$. For GPs, the candidate points are typically randomly sampled but then further optimized directly using the acquisition function. In SMAC, candidate points are sampled using a combination of random search and local search in the good regions found by the random forest. For TPE, the candidate points are sampled directly from the density of “good” points, $g(h)$.
3. **Acquisition function:** The acquisition function $a : \mathcal{H} \rightarrow \mathbb{R}$ scores and selects the candidate points using the surrogate model. One of the most popular acquisition functions is expected improvement (EI): $a(h) = \mathbb{E}[\max(p(s|h) - f(h_{best}), 0)]$, where $f(h_{best})$ is the value of the best observation so far (31). The point that maximizes the acquisition function is selected as the next sample to evaluate $h = \arg \max_{\tilde{h} \in \tilde{\mathcal{H}}} a(\tilde{h})$. Other popular acquisition functions include the probability of improvement (33) and upper confidence bound (52).

The BO process thus operates by first updating the surrogate model with existing data, and then sampling a set of promising candidate points. Using the surrogate model, the acquisition function scores each candidate point and selects the best point for evaluation. The new point and observed value are appended to available observations, and the cycle continues.

A.2 RELATED WORKS

Bayesian optimization. At its core, Bayesian Optimization relies on probabilistic modeling. The most widely adopted technique is the Gaussian Processes (GP) due to their flexibility and analytical tractability (46, 49). Recent works have sought to enhance their expressiveness, evident in deep kernel GP (27, 62) and manifold GPs (10). On another front, Bayesian neural networks have been explored as expressive and computationally efficient variants (50, 51). Alternatively, traditional ensemble approaches, including Random Forests, (29) have been used to obtain empirical uncertainty estimations. Tree-structured Parzen Estimator (TPE) (6) is an alternate approach that models $p(h|s)$ and has been widely adopted in practical applications, including in Optuna (1) and HyperOpt (7). Recent trends have also leaned towards Transformers (12, 38) as surrogate models. Of particular note is the research that delves into in-context learning for BO of molecules in (45). While this work primarily focused on the surrogate model, we introduce novel methods for LLM enhancement of multiple components of BO and conduct a systematic investigation to understand the performance gains offered by this integration.

Transfer learning for BO. Recently, many works have explored transfer learning to generalize learnings from similar domains. Prominent among these are multitask GPs (22, 54, 63). This class of methods is designed to optimize several related black-box functions by sharing information across tasks and leveraging common structures or patterns. Other approaches have sought to

transfer learnings from previously optimized functions to new functions (4, 44). However, these approaches are limited as they only consider inductive transfer over a fixed search space, i.e. all tasks share the same set of inputs. More recently, (12) introduced a large-scale pretrained Transformer for meta-learning across tasks with different search spaces. In many black-box optimization settings, collecting prior optimization results from similar optimization problems is resource-intensive and might not be feasible for certain applications. In our work, we explore a lightweight alternative by harnessing unstructured domain knowledge contained in generalist LLMs, which does not require dedicated pretraining and structure results from related optimization problems.

B COMPLETE PROMPTS

In this section, we include the complete prompts used to query the LLMs for each component of BO, including:

1. Zero-shot prompts for warmstarting with ► **No Context** (Figure 9); ► **Partial Context** (Figure 10); and ► **Full Context** (Figure 11).
2. ICL prompts for ► **discriminative surrogate model** (Figure 12) and ► **generative surrogate model** (Figure 13).
3. ICL prompts for target value conditioned **candidate sampling** in Figure 14.

You are assisting me with automated machine learning using **model**. I’m exploring a subset of hyperparameters detailed as: **configurations, type, and ranges**. Please suggest **num recommendations** diverse yet effective configurations to initiate a Bayesian Optimization process for hyperparameter tuning. You mustn’t include “None” in the configurations. Your response should include a list of dictionaries, where each dictionary describes one recommended configuration.

Figure 9: Prompt for warmstarting with **No Context**.

You are assisting me with automated machine learning using **model** for a **task** task. The **task** performance is measured using **metric**. The dataset has **number of samples** samples with **num features** total features, of which **number of total features** are numerical and **number of categorical variables** are categorical. **[statistical information]** I’m exploring a subset of hyperparameters detailed as: **configuration and type**. Please suggest **number of recommendations** diverse yet effective configurations to initiate a Bayesian Optimization process for hyperparameter tuning. You mustn’t include ‘None’ in the configurations. Your response should include a list of dictionaries, where each dictionary describes one recommended configuration.

Figure 10: Prompt for warmstarting with **Partial Context**.

You are assisting me with automated machine learning using **model** for a **task** task. The **task** performance is measured using **metric**. The dataset has **number of samples** samples with **number of features** total features, of which **number of continuous features** are numerical and **number of categorical features** are categorical. **statistical information** I’m exploring a subset of hyperparameters detailed as: **configuration and type**. Please suggest **number of recommendation** diverse yet effective configurations to initiate a Bayesian Optimization process for hyperparameter tuning. You mustn’t include ‘None’ in the configurations. Your response should include a list of dictionaries, where each dictionary describes one recommended configuration.

Figure 11: Prompt for warmstarting with **Full Context**.

The following are examples of the performance of a **model** measured in **metric** and the corresponding model hyperparameter configurations. The model is evaluated on a tabular **task** containing **number of classes** classes. The tabular dataset contains **number of samples** samples and **number of features** features (**number of categorical features** categorical, **number of continuous features** numerical). Your response should only contain the predicted accuracy in the format **## performance ##**.

Hyperparameter configuration: **configuration 1**
 Performance: **performance 1**

...

Hyperparameter configuration: **configuration n**
 Performance: **performance n**

Hyperparameter configuration: **configuration to predict performance**
 Performance:

Figure 12: Prompt for **discriminative surrogate model**.

The following are examples of the performance of a **model** measured in **metric** and the corresponding model hyperparameter configurations. The model is evaluated on a tabular **task** containing **number of classes** classes. The tabular dataset contains **number of samples** samples and **number of features** features (**number of categorical features** categorical, **number of continuous features** numerical). The performance classification is 1 if the configuration is in the best-performing 25.0% of all configurations, and 0 otherwise. Your response should only contain the predicted performance classification in the format **## performance classification ##**.

Hyperparameter configuration: **configuration 1**
 Classification: **classification 1**

...

Hyperparameter configuration: **configuration n**
 Classification: **classification n**

Hyperparameter configuration: **configuration to classify**
 Classification:

Figure 13: Prompt for **generative surrogate model**.

The following are examples of the performance of a **model** measured in **metric** and the corresponding model hyperparameter configurations. The model is evaluated on a tabular **task** containing **number of classes** classes. The tabular dataset contains **number of samples** samples and **number of features** features (**number of categorical features** categorical, **number of continuous features** numerical). The allowable ranges for the hyperparameters are: **configuration and type**. Recommend a configuration that can achieve the target performance of **observed score**. Do not recommend values at the minimum or maximum of allowable range, do not recommend rounded values. Recommend values with the highest possible precision, as requested by the allowed ranges. Your response must only contain the predicted configuration, in the format **## configuration ##**.

Performance: **performance 1**
 Hyperparameter configuration: **configuration 1**

...

Performance: **performance n**
 Hyperparameter configuration: **configuration n**

Performance: **performance used to sample configuration**
 Hyperparameter configuration:

Figure 14: Prompt for **candidate sampling**.

C DETAIL OF EXPERIMENTAL PROCEDURES

Benchmark. We utilize Bayesmark (55) as a continuous HPT benchmark.³ We include all 5 included datasets and 5 ML models, including RandomForest, SVM, DecisionTree, MLP, and AdaBoost. Additionally, we introduce 3 proprietary and 3 synthetic datasets into the benchmark. These are datasets for which the LLM would not have seen during pretraining, and thus used to address any memorization concerns. This makes a total of 55 tasks, with each task defined as the (dataset, model) pair. We execute all tasks using five different seeds for 25 trials, ensuring that all models share the same initialization for each seed. This approach guarantees consistency across results. For classification and regression tasks, the scoring function is accuracy and MSE, respectively.

Hyperparameter space. The space of each hyperparameter is given by:

- SVM: {C: [1, 1e3], γ : [1e-4, 1e-3], tolerance: [1e-5, 1e-1]}
- DecisionTree: {max_depth: [1, 15], min_samples_split: [0.01, 0.99], min_samples_leaf: [0.01, 0.49], min_weight_fraction_leaf: [0.01, 0.49], max_features: [0.01, 0.99], min_impurity_decrease: [0.0, 0.5]}
- RandomForest: {max_depth: [1, 15], min_samples_split: [0.01, 0.99], min_samples_leaf: [0.01, 0.49], min_weight_fraction_leaf: [0.01, 0.49], max_features: [0.01, 0.99], min_impurity_decrease: [0.0, 0.5]}
- MLP: {hidden_layer_sizes: [50, 200], alpha: [1e-5, 1e1], batch_size: [10, 250], learning_rate_init: [1e-5, 1e-1], power_t: [0.1, 0.9], tol: [1e-5, 1e-1], momentum: 0.001, 0.999], validation_fraction: [0.1, 0.9]}
- AdaBoost: {n_estimators: [10, 100], learning_rate: [1e-4, 1e1]}

Setting of LLAMBO. For our instantiation of LLAMBO, we sample $M = 20$ candidate points, and set the exploration hyperparameter to $\alpha = -0.1$. For the surrogate model, we sample $K = 10$ MC predictions to compute the empirical estimates.

Private & Synthetic datasets. We include three proprietary datasets SEER (18), MAGGIC (43), and CUTRACT (40) as additional datasets for evaluation. Additionally, we included three synthetic datasets based on the complex multimodal functions, specifically: Rosenbrock, Griewank, and KTablet (see (58) for full simulation parameters). We selected the input dimension as 15, where each dimension is uniformly sampled in the range of [0, 1]. Subsequently, we used the designated functions in (58) to generate the corresponding output.

Baselines. We select the following baselines:

- SKOpt (GP-based) (41): We used the library implementation https://scikit-optimize.github.io/stable/modules/generated/skopt gp_minimize.html. Additionally, we optimize the acquisition of candidates for better results, `acq_optimizer = lbfgs`.
- GP (Deep Kernel Learning) (63): We use the implementation of GPytorch https://docs.gpytorch.ai/en/stable/examples/06_PyTorch_NN_Integration_DKL/KISSGP_Deep_Kernel_Regression_CUDA.html in combination with the optimization of acquisition function used in BoTorch <https://botorch.org/docs/acquisition> for a better performance.
- DNGO: We used a public implementation <https://github.com/automl/pybnn>.
- SMAC3 (34): We used public implementation <https://github.com/automl/SMAC3>.
- Turbo (20): We used the implementation found in <https://github.com/uber-research/TuRBO>.
- HEBO (14): We used the available pip version of HEBO <https://pypi.org/project/HEBO/>.
- Optuna (1). We consider the implementation of <https://optuna.org/>. We used the multi-variate version, which was found to have better performance in (21).
- TPE (58). We incorporated an additional implementation of TPE, essentially a heavily optimized variant of TPE designed to achieve competitive results <https://github.com/nabenabe0928/tpe>.

³<https://github.com/uber/bayesmark/tree/8c420e935718f0d6867153b781e58943ecaf2338>

D GENERATIVE SURROGATE MODEL

In introducing TPE, (6) showed that the EI of each point is defined as such:

$$EI(h) \propto \left(\gamma + \frac{g(h)}{l(h)}(1 - \gamma) \right)^{-1}$$

In other words, to maximize EI, we would like h that has high probability under $l(h)$ and low probability under $g(h)$. By simple application of Bayes rule, we can rewrite this as:

$$\begin{aligned} \left(\gamma + \frac{g(h)}{l(h)}(1 - \gamma) \right)^{-1} &= \left(\gamma + \frac{p(h|s > \tau)}{p(h|s \leq \tau)}(1 - \gamma) \right)^{-1} \\ &= \left(\gamma + \frac{p(s > \tau|h)p(s \leq \tau)}{p(s \leq \tau|h)p(s > \tau)}(1 - \gamma) \right)^{-1} \\ &= \left(\gamma + \frac{p(s > \tau|h)p(s \leq \tau)}{p(s \leq \tau|h)} \right)^{-1} \\ &= \left(\frac{\gamma}{p(s \leq \tau|h)} \right)^{-1} \\ &= \gamma^{-1} p(s \leq \tau|h) \end{aligned}$$

Thus, the expression is equivalently rewritten as $\gamma^{-1} p(s \leq \tau|h)$, which is proportional to $p(s \leq \tau|h)$, i.e. the probability of h belonging to the *good* points.

E ADDITIONAL RESULTS

E.1 ADDITIONAL WARMSTARTING RESULTS

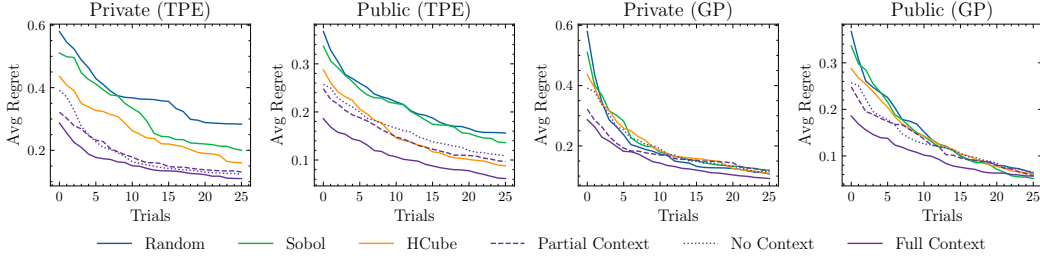


Figure 15: Fine-grained warmstarting results.

As part of our investigation into warmstarting, we investigated the effect of varying the amount of information provided in the zero-shot prompts on the quality of warmstart initialization. Specifically, **► No Context**, **► Partial Context** and **► Full Context**. We evaluate the effectiveness of warmstarting by evaluating the search performance of GP and TPE under different initialization. In Figure 15, we plot average regret across tasks for both BO models. We observe similar trends, that increasing the informativeness of the prompts led to improved search performance.

E.2 LLAMBO WITH GENERATIVE SURROGATE MODEL

Due to budgetary constraints, we did not evaluate LLAMBO with both proposed surrogate models in Section 6. To determine the stronger surrogate model for our end-to-end evaluations, we tested both methods in a constrained setting. This meant assessing both models on a single run across all 25 tasks within the public Bayesmark benchmark. The outcomes of this preliminary evaluation are depicted in Figure 16. Our findings indicated that the LLAMBO with a discriminative surrogate model outperformed its counterpart. Consequently, we opted for the discriminative surrogate model for a comprehensive evaluation. However, it’s worth noting that the LLAMBO using a generative surrogate model showcased competitive results when compared with baseline measures. Both approaches exhibited swift search and convergence in the initial trials, especially when $n < 10$. The generative instantiation was a close second until the last few trials.

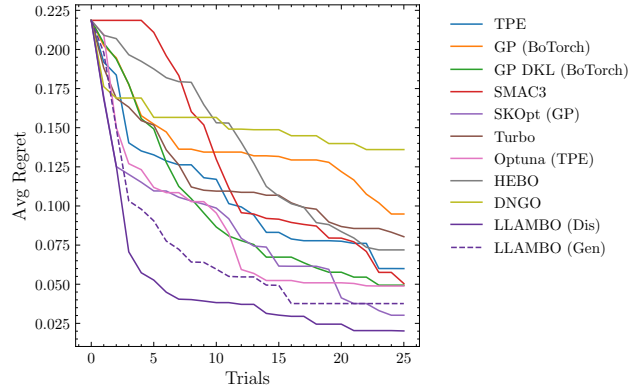


Figure 16: **End-to-end performance of LLaMBO (generative surrogate model).** (Left) Average regret on public datasets and (Right) private and synthetic datasets evaluated on Bayesmark’s datasets.

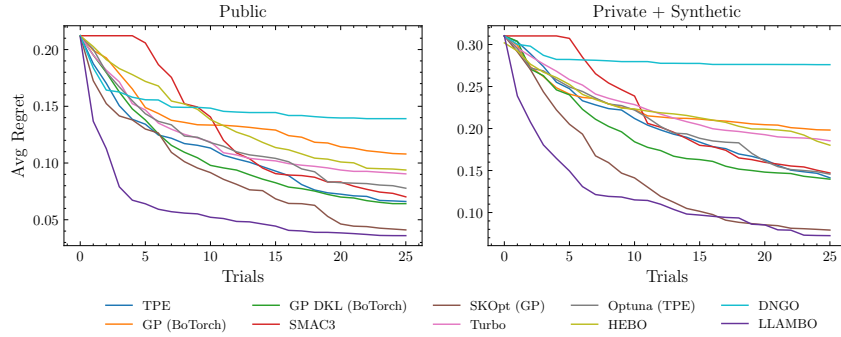


Figure 17: **End-to-end performance of LLaMBO.** (Left) Average regret on public datasets and (Right) private and synthetic datasets aggregated on all tasks.

Drawing definitive conclusions from a single seed can be challenging. However, we postulate that our model’s generative version might exhibit sensitivity to the τ hyperparameter, which dictates the boundary between good and bad points. A recent study on inherent LLM biases in ICL by (66) underscored the majority label bias—a tendency of the model to favor the majority label in the given few-shot examples. This bias is intrinsically tied to our generative surrogate model’s design, where τ determines the proportion of points labeled as good versus bad. We see a thorough examination of this potential bias, an in-depth analysis of the τ hyperparameter’s sensitivity, and the exploration of bias-correction techniques as key future research avenues to fully explore the generative surrogate model’s capabilities.

E.3 ADDITIONAL RESULTS FOR LLaMBO

In this section, we include additional results to supplement our end-to-end evaluation.

Additional baselines. We include additional baselines in Figure 17, including an optimized version of TPE from (58), DNGO (a Bayesian neural network approach (50)), Turbo (20) (a GP approach that identifies ‘trusted regions’ of the input space to search for improvements), and HEBO (15). This presents a more comprehensive evaluation against a wide array of BO approaches.

Search performance across ML models. In Tables 1 and 2 we compare the tuning performance of BO methods for different types of ML models. We show the average rank achieved by methods at the end of each search. Although LLaMBO consistently demonstrates the best overall performance, it exhibits model-dependent variability. Notably, LLaMBO excels in tuning DecisionTree and RandomForest across both public and private benchmarks. However, it does less well on SVMs. The underlying cause of this remains speculative, but one plausible explanation is the inherent characteristics of the black-box function being optimized. This sensitivity and such nuances are common to

Table 1: Average rank (\downarrow) achieved for different ML methods on public datasets.

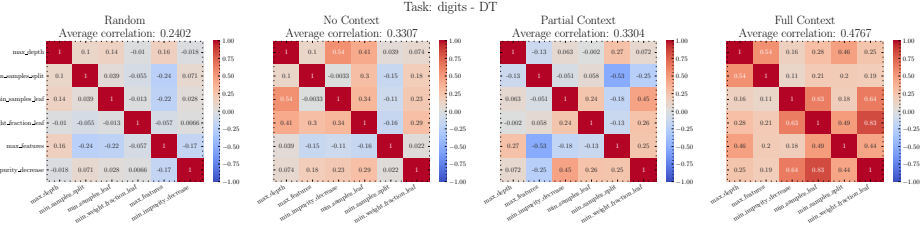
| | DT | MLP | RF | SVM | ADA |
|------------------|-------------|-------------|-------------|-------------|-------------|
| TPE | 6.16 | 5.12 | 5.34 | 4.64 | 5.52 |
| GP (BoTorch) | 6.72 | 5.62 | 5.94 | 6.06 | 4.74 |
| GP DKL (BoTorch) | 4.30 | 4.63 | 5.52 | 5.60 | 6.26 |
| SMAC3 | 5.82 | 6.42 | 5.40 | 5.66 | 6.02 |
| SKOpt (GP) | 3.66 | 4.40 | 4.90 | 4.84 | 5.12 |
| Turbo | 5.86 | 4.40 | 5.60 | 5.38 | 5.78 |
| Optuna (TPE) | 6.58 | 5.34 | 5.48 | 5.08 | 5.08 |
| HEBO | 6.14 | 4.88 | 5.10 | 6.30 | 5.72 |
| DNGO | 7.74 | 8.62 | 8.08 | 6.62 | 7.14 |
| LLAMBO | 2.02 | 5.06 | 3.64 | 4.82 | 3.62 |

Table 2: Average rank (\downarrow) achieved for different ML methods on private and synthetic datasets.

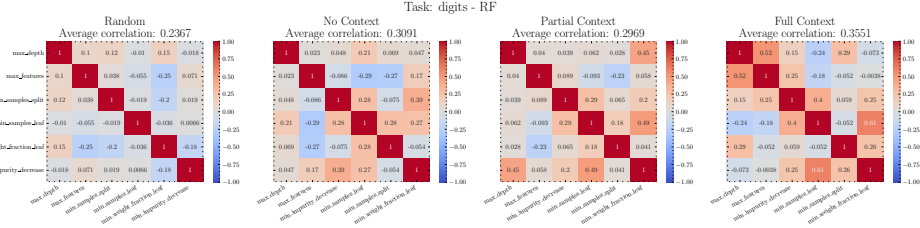
| | DT | MLP | RF | SVM | ADA |
|------------------|-------------|-------------|-------------|-------------|-------------|
| TPE | 4.85 | 4.83 | 4.95 | 4.83 | 3.98 |
| GP (BoTorch) | 6.70 | 6.18 | 7.08 | 7.10 | 5.45 |
| GP DKL (BoTorch) | 4.78 | 4.25 | 4.60 | 5.05 | 5.60 |
| SMAC3 | 5.12 | 5.33 | 5.13 | 6.15 | 5.40 |
| SKOpt (GP) | 4.83 | 4.98 | 4.52 | 2.32 | 4.95 |
| Turbo | 5.80 | 5.07 | 5.77 | 6.10 | 4.88 |
| Optuna (TPE) | 4.98 | 5.75 | 5.37 | 5.12 | 5.52 |
| HEBO | 6.50 | 6.33 | 6.25 | 6.13 | 5.15 |
| DNGO | 7.83 | 8.17 | 9.12 | 7.32 | 7.62 |
| LLAMBO | 3.35 | 4.10 | 2.08 | 4.88 | 6.45 |

all BO techniques, given their sensitivities to black-box functions with different attributes (e.g. the choice of kernel directly affects the effectiveness of GP for specific functions) (19). Exploring the characteristics of black-box functions where our method shines is a crucial avenue for future research and remains beyond the scope of our current study.

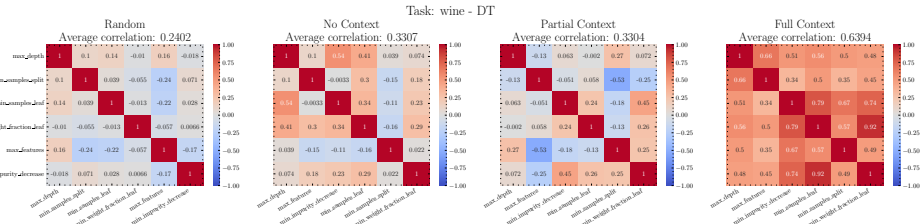
Individual task results. We plot individual task results by optimization metric (Figure 19), regret (Figure 20), and average rank of BO methods (Figure 21) (all results are averaged over 5 runs).



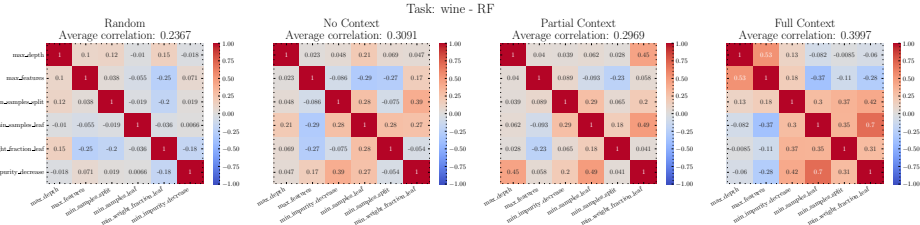
(a) Task: DT on Digits.



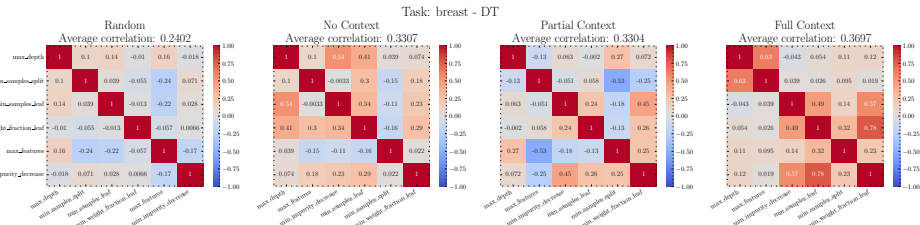
(b) Task: RF on Digits.



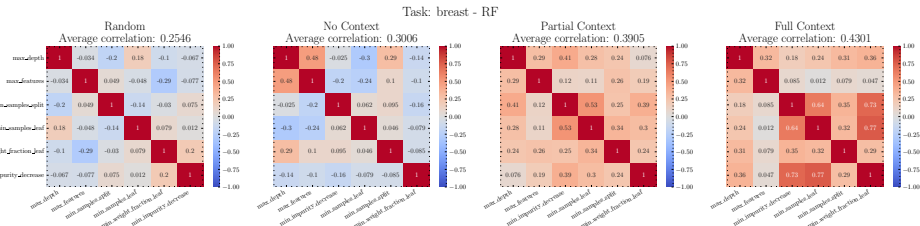
(c) Task: DT on Wine.



(d) Task: RF on Wine.



(e) Task: DT on Breast.



(f) Task: RF on Breast.

Figure 18: **Comparison of correlations between sampled initializations.** Correlation matrix calculated on 50 initialization sampled for each task.

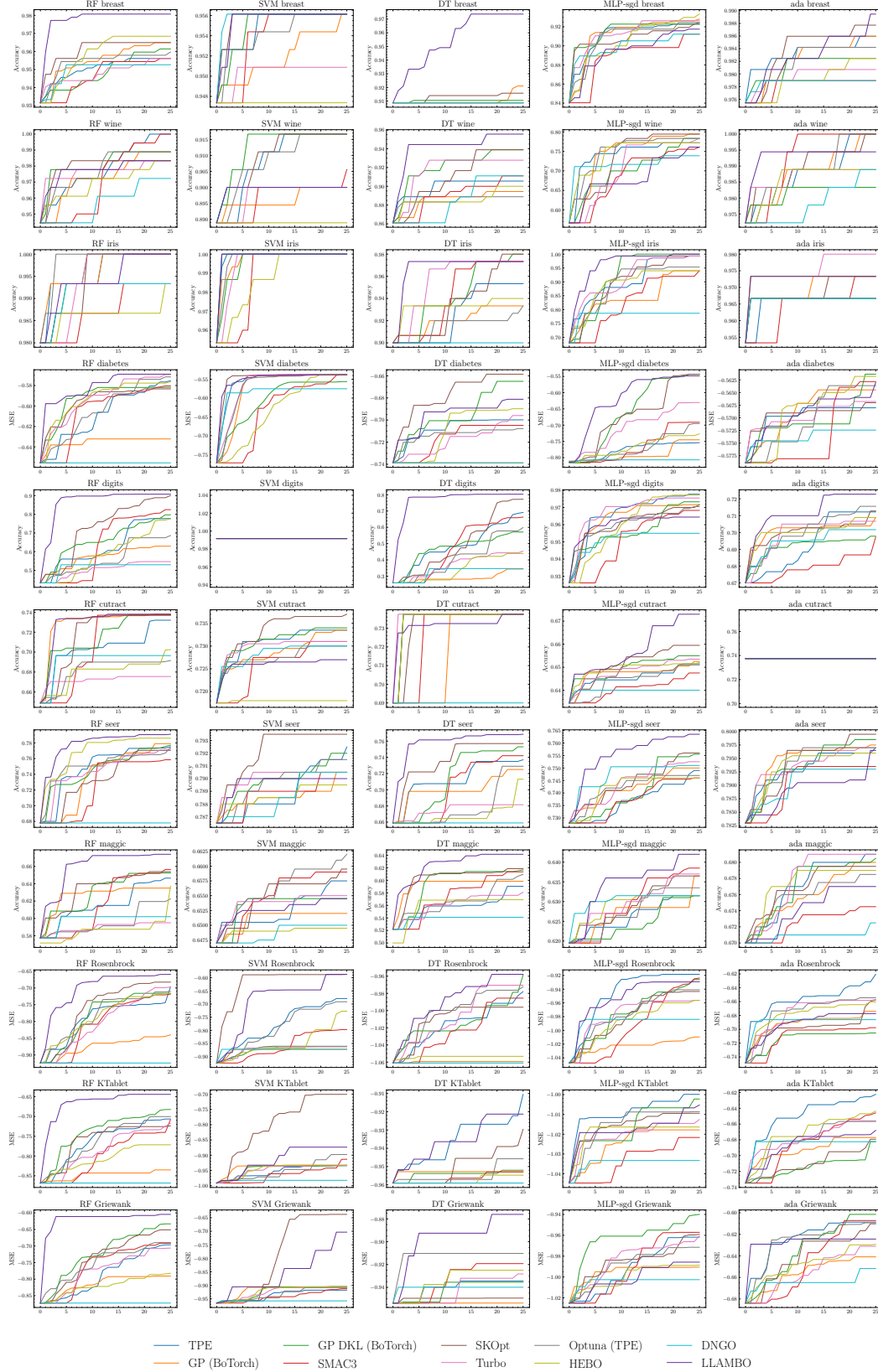


Figure 19: **Individual HPT task results.** Evaluations according to task metrics, i.e. accuracy (\uparrow) for classification tasks, and *negative* MSE (\uparrow) for regression tasks. Results averaged over 5 runs.

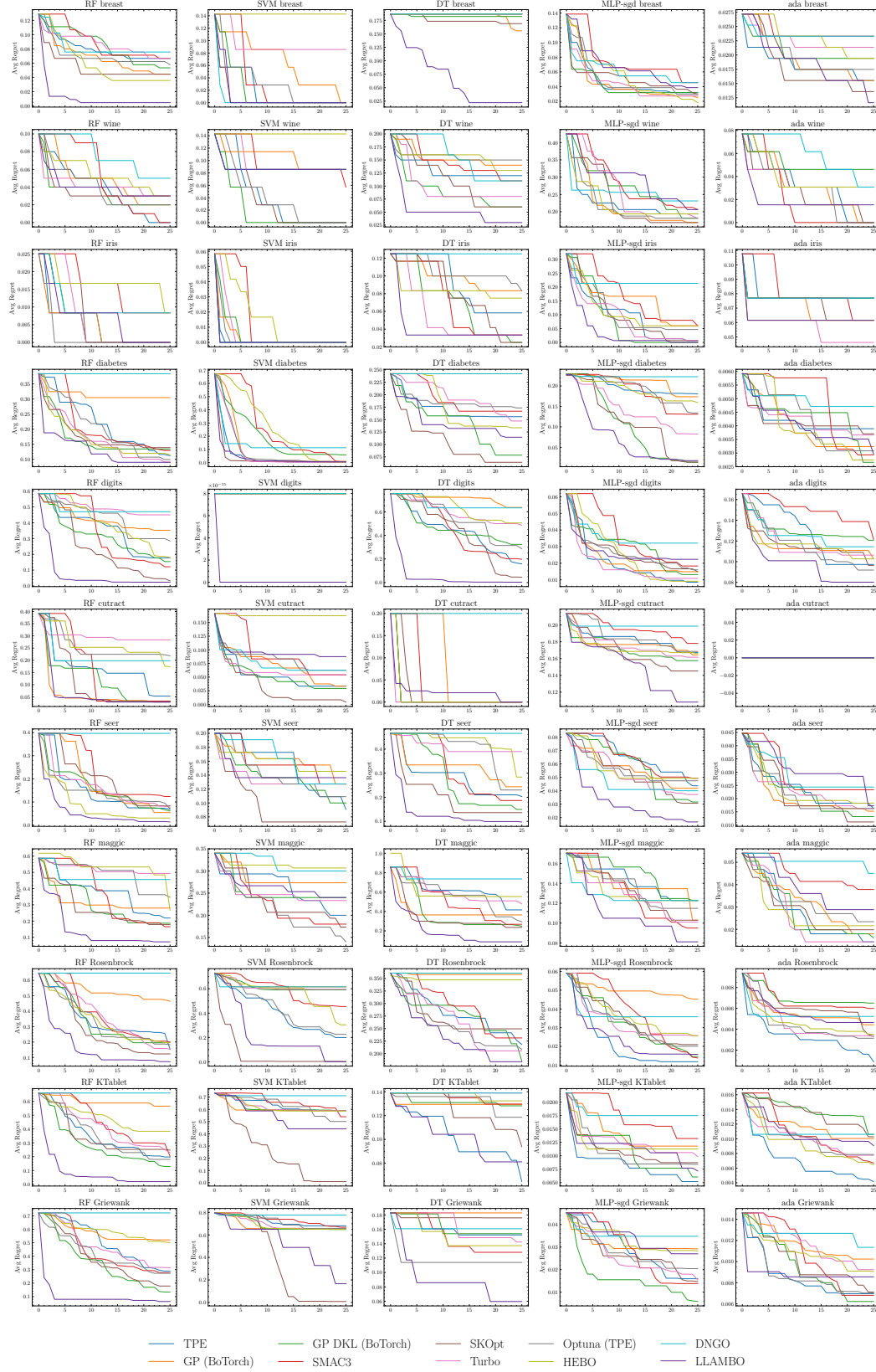


Figure 20: **Individual HPT task results.** Evaluations according to normalized regret (\downarrow), averaged over 5 runs.

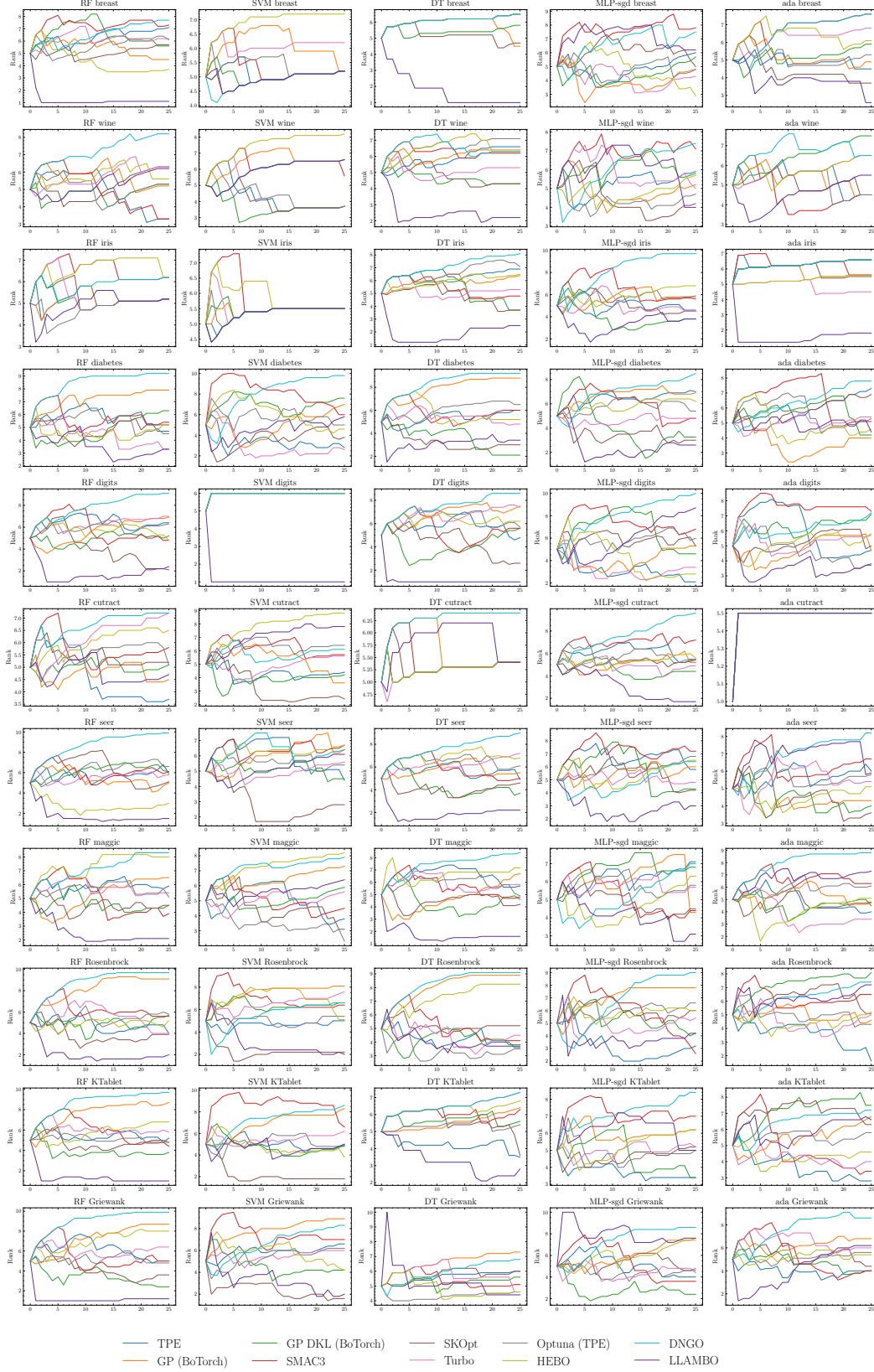


Figure 21: **Individual HPT task rank.** Evaluations according to average rank (\downarrow) during each search, averaged over 5 runs.